Metabolic Engineering Communications 8 (2019) e00084

Contents lists available at ScienceDirect

Metabolic Engineering Communications

journal homepage: www.elsevier.com/locate/mec

Enhancement of himastatin bioproduction via inactivation of atypical repressors in *Streptomyces hygroscopicus*

Yunchang Xie[a], Qinglian Li[a], Xiangjing Qin[a], Jianhua Ju[a,b,*], Junying Ma[a,*,**]

[a] CAS Key Laboratory of Tropical Marine Bioresources and Ecology, Guangdong Key Laboratory of Marine Materia Medica, Research Network for Applied Microbiology Center for Marine Microbiology, South China Sea Institute of Oceanology, Chinese Academy of Sciences, Guangzhou 510301, China
[b] College of Earth Sciences, University of Chinese Academy of Sciences, Beijing 100049, China

ARTICLE INFO

Keywords:
Himastatin
Streptomyces hygroscopicus
Repressor
Biosynthesis
Bioproduction

ABSTRACT

Three atypical regulatory genes, *hmtABD* have been discovered within the himastatin biosynthetic gene cluster (BGC) in *Streptomyces hygroscopicus* ATCC 53653 and the roles of their products have been identified. HmtA and HmtD do not show any structurally distinct features characteristic of regulatory function yet were shown to play important repressive and stimulatory roles, respectively, related to himastatin biosynthesis. HmtB encodes a conserved acetylglutamate kinase; new member of this family serves as repressor of secondary metabolism. Through repressive networks engineering, the limiting functions of HmtA and HmtB along with the activating functions of HmtD in the himastatin BGC have been identified for the first time by gene activation, qPCR, RT-PCR and HPLC studies of selected mutant strains; two of these mutant strains (Δ*hmtA* and Δ*hmtB*) produced himastatin in titers (19.02 ± 1.2 μg/mL, 9.9 folds and 30.40 ± 0.83 μg/mL, 15.8 folds) far exceeding those of the wild-type (WT) producer. Overall, this work provides significant insight into secondary metabolic regulatory mechanisms in *Streptomyces*. These efforts also highlight and validate a new strategy enabling expanded exploitation of cyclopeptidic natural products such as himastatin that demonstrate exciting antimicrobial and antitumor potentials.

1. Introduction

Himastatin, a symmetrical dimeric cyclohexadepsipeptide, was first identified in 1990 from the culture broth of *Streptomyces hygroscopicus* ATCC 53653 (Kumar and Goodfellow, 2008; Lam et al., 1990; Leet et al., 1990). Each monomer consists of a D-valine, a L-α-hydroxyisovaleric acid, a (*3R*, *5R*)-5-hydroxypiperazic acid, a L-leucine, a D-threonine and a (*2R*, *3aR*, *8aR*)-3a-hydroxyhexahydropyrrolo[2, 3b]indole 2-carboxylic acid subunit; monomer dimerization is achieved by virtue of a regioselective C–C biphenyl linkage (Fig. 1) (Leet et al., 1996).

Himastatin has shown antimicrobial activity against a number of Gram-positive bacteria in vitro (Lam et al., 1990). The ability of himastatin to cure mice inoculated with P388 leukemia and B16 melanoma cells reflects the compound's significant anticancer activities (Lam et al., 1990). By virtue of its striking molecular structure and potent biological activities, himastatin has served as a valuable tool for new approaches to infectious disease and cancer treatments while also representing a high value target for synthetic chemists as reflected by Danishefsky's total synthesis in 1998 (Kamenecka and Danishefsky, 1998a,1998b,2001).

The 45 kb himastatin (*hmt*) biosynthetic gene cluster (BGC) was identified (Fig. 2) in 2011 and himastatin's construction elucidated using a series of gene inactivation and complementation experiments along with structural characterization of assorted intermediates (Ma et al., 2011). From these efforts evolved a biosynthetic sequence in which himastatin is constructed via a nonribosomal peptide synthetase (NRPS) assembly pathway (Ma et al., 2011). The NRPS assembly line, consisting of initial HmtI and HmtFKL, incorporates each of the six amino acids composing one monomer and cyclizes the hexapeptide to generate the cyclohexadepsipeptide monomer. Subsequently, himastatin construction entails two cytochrome P450 enzymes, HmtTN, which then catalyze post-NRPS modification of stereospecific epoxidation and hydroxylation, and the critical cytochrome P450 enzyme HmtS installs

* Corresponding author at: CAS Key Laboratory of Tropical Marine Bioresources and Ecology, Guangdong Key Laboratory of Marine Materia Medica, Research Network for Applied Microbiology Center for Marine Microbiology, South China Sea Institute of Oceanology, Chinese Academy of Sciences, Guangzhou 510301, China.
** Corresponding author.
E-mail addresses: jju@scsio.ac.cn (J. Ju), majunying@scsio.ac.cn (J. Ma).

https://doi.org/10.1016/j.mec.2018.e00084
Received 27 June 2018; Received in revised form 8 November 2018; Accepted 10 December 2018

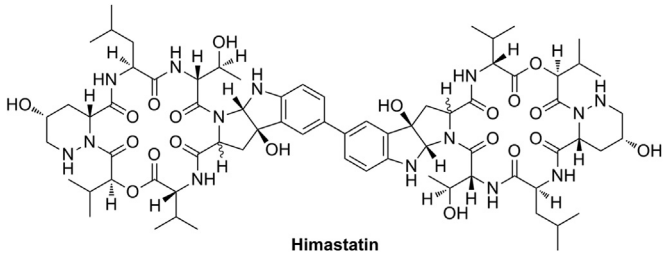

Fig. 1. Chemical structure of himastatin.

the distinctive biaryl C–C linkage to generate intact himastatin (Ma et al., 2011; Zhang et al., 2013). Additionally, *hmtCM* encode the enzymes responsible for the biosynthesis of (3R, 5R)-5-hydroxypiperazic acid precursor (Du et al., 2017), *hmtQR* encode two transporters responsible for himastatin transmembrane efflux, *hmtEOP* encode unknown function proteins (hypothetical) that gene inactivation studies suggest have no direct influence on himastatin biosynthesis (Ma et al., 2011). Besides the aforementioned genes, three other genes *hmtABD* located in the upstream region of the *hmt* cluster have not yet been rigorously evaluated (Fig. 2). Previous bioinformatics analyses indicated that *hmtA* encodes a MerR family transcriptional regulator and *hmtD* encodes an uncharacterized regulator. The *hmtB* gene encodes a putative acetylglutamate kinase; comparisons to other such enzymes suggested a regulatory role. On the strength of these findings we posited that HmtABD might all regulate, or assist in regulating, himastatin biosynthesis.

As is widely known, bioproduction of secondary metabolites in *Streptomyces* is a process controlled by regulatory elements commonly grouped within BGCs. Thus, secondary metabolic pathways can readily respond to disparate environmental and physicochemical factors such as nutrient levels, pH, temperature and so on, readily coordinating the host's growth and development (Bibb, 2005; Li et al., 2017; Martin and Liras, 2010; Olano et al., 2008; van Wezel and McDowall, 2011). Especially, functional repressors are ideal targets for inactivation. Alleviating points of building block limitation or restriction of enzymatic activity within biosynthetic pathways has been proven to significantly enhance secondary metabolite titers (Baltz, 2016; Li et al., 2017). This strategy, termed “regulatory networks engineering” is widely applied to improve antibiotic bioproduction; some examples include the production of tylosin, pimaricin, actinorhodin, undecylprodigiosin, A201A and kasugamycin (Mendes et al., 2007; Sola-Landa et al., 2003; Stratigopoulos and Cundliffe, 2002; Stratigopoulos et al., 2002; Zhu et al., 2016; Zhu et al., 2012). Now enabled by the identification of the *hmt* cluster and putative characterization of its machinery, we report: 1) the identification of three genes encoding for atypical regulators within the himastatin BGC: *hmtABD*, 2) HmtA and HmtD do not appear to contain functional regulatory domains but work as a repressor (HmtA) and the only activator (HmtD) involved in himastatin biosynthesis respectively, 3) HmtB is the first identified acetylglutamate kinase type repressor in himastatin biosynthesis, 4) 9.9-folds (19.02 ± 1.2 μg/mL,) and 15.8-folds (30.40 ± 0.83 μg/mL) improvements in himastatin bioproduction for inactivation mutants Δ*hmtA* and Δ*hmtB* – these data lay a solid foundation for further preclinical studies with himastatin.

2. Materials and methods

2.1. Bacterial strains, plasmids, and media

S. hygroscopicus ATCC 53653 (WT) was obtained from American Type Culture Collection (ATCC). *Escherichia coli* DH5α was used for general cloning. *E.coli* ET12567/pUZ8002 was used for transferring DNA into *Streptomyces* by conjunction. *E.coli* BW25113/pIJ790 was used as the host for PCR-targeting. Plasmid pIJ773 was used as template to amplify the *aac(3)IV* apramycin resistance cassette. *S. hygroscopicus* and its derivatives were grown at 30 °C on ISP4 agar supplemented with 0.1% peptone and 0.05% yeast extract (modified ISP4) for sporulation; in liquid fermentation medium (1% fish powder, 2% glycerol, 0.5% $CaCO_3$, 0.5% yeast extract, pH 7.2) for himastatin production; in liquid TSB for genomic DNA extraction. All *E. coli* strains were grown on agar or liquid Luria-Bertani (LB) medium at 30 °C or 37 °C. When needed, antibiotics were supplemented as the following concentrations: apramycin (Apr), 50 μg/mL in LB medium for *E. coli*, 25 μg/mL in modified ISP4 for *S. hygroscopicus*; kanamycin (Kan), 50 μg/mL in LB medium for *E. coli*; ampicillin (Amp), 100 μg/mL in LB medium for *E. coli*; chloramphenicol (Cml), 25 μg/mL in LB medium for *E. coli*.

2.2. DNA isolation, manipulation, sequencing, and bioinformatics analysis

Routine DNA manipulation with *E. coli* and recombinant DNA techniques in *Streptomyces* species were performed as described previously (Ma et al., 2011). Routine DNA sequencing was carried out by The Beijing Genomics Institute (BGI) (Shenzhen, China). Primers were synthesized by Sangong (Shanghai, China). Protein secondary structure predictions were performed using the NCBI BLAST program (https://blast.ncbi.nlm.nih.gov/Blast.cgi). The multiple sequence alignments and homology comparisons were performed using Clustal W and BLAST software.

2.3. Gene inactivation of hmtABD in S. hygroscopicus ATCC 53653 to construct the mutant strains

Gene inactivation of targeting specific genes within the himastatin biosynthetic gene cluster were performed as described previously (Ma et al., 2011). Generally, cosmid E4 was used to inactivate the *hmtA*, *hmtB* and *hmtD* genes in the himastatin biosynthetic gene cluster; specific primers used to inactivate these genes are listed in Table S1. That each of the mutated cosmids correlated to the desired targeted gene was confirmed by PCR through the use of primers designed to bind 300–500 bp outside of the disruption region as listed in Table S2. The three mutated cosmids produced in this manner were introduced into non-methylating *E. coli* ET12567/pUZ8002 for conjugation. The double crossover mutants showing the kanamycin-sensitive and apramycin-resistant ($Kan^S Apm^R$) phenotype were further confirmed by PCR with use of the primers detailed in Table S1 (for gel analyses see Fig. S3–S5). Ultimately, Three *S. hygroscopicus* ATCC 53653 mutant strains—Ju1501 (Δ*hmtA*), Ju1502 (Δ*hmtB*), Ju1504 (Δ*hmtD*)—were obtained and subsequently used to assess the role and importance of each individual gene in himastatin biosynthesis.

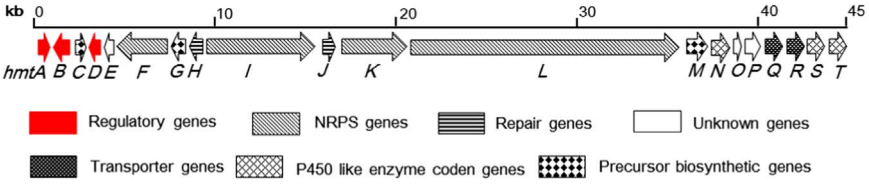

Fig. 2. Gene organization of the himastatin (*hmt*) biosynthetic gene cluster in *S. hygroscopicus* ATCC 53653.

To construct the complementation mutant of Δ*hmtD*, *hmtD* was amplified from E4 cosmid with the primers listed in Table S1. The fragments were cloned into pCR2.1 vector for sequencing. Then *hmtD* was digested with *Nde*I and *Spe*I and then cloned into pSET152AKE vector to generate pSET152AKE-*hmtD*, which was also digested with *Nde*I and *Spe*I enzyme. The construction process of Δ*hmtD::hmtD* was the same as we previous descripted (Ma et al., 2011). The fermentation and HPLC analysis of Δ*hmtD::hmtD* was also the same as aforementioned (Ma et al., 2011).

2.4. Quantitative analysis of himastatin bioproduction using S. hygroscopicus ATCC 53653WT and mutant strains

S. hygroscopicus WT and mutant strains were grown on M-ISP4 agar plates for 7 d at 30 °C. A suitable portion of spores was inoculated into 50 mL fermentation medium in an Erlenmeyer flask (250 mL) and incubated at 30 °C and 200 rpm for 7 d. To obtain statistically significant results, three independent exconjugants of each recombinant strain were selected and fermentations were repeated at least three times independently. The resulting fermentation broth was extracted with ethyl acetate (1 ×100 mL), and the solvent was removed in vacuum. The extracts were dissolved in 1 mL CH_3OH and centrifuged at 13,000*g* for 10 min, and 30 μl of supernatant was subjected to HPLC analysis following the previously described system (Ma et al., 2011).

In order to calculate the yields of himastatin in the mutants and the wild type S. *hygroscopicus* ATCC 53653, a quantitative curve was established based on the relationship of integral area and the weight of himastatin. To quantitatively analyze himastatin titers in the Δ*hmtA* and Δ*hmtB* mutant strains and that of the WT strain, extracts of the mutant strains were diluted 10 times and then subjected to HPLC alongside analogously prepared WT-derived extract. The titers of himastatin in different strains were calculated based on the established standard himastatin curve. The magnitude of increased (relative to WT) himastatin titers for both mutants were shown in histogram. The *t*-test was used in the quantitative calculation of himastatin titers in different strains.

2.5. RT-PCR and qPCR analysis of S. hygroscopicus ATCC 53653WT and mutant strains

S. hygroscopicus ATCC 53653 WT and mutant strains incubated in fermentation medium were harvested and flash-frozen in liquid N_2. Frozen mycelia pellets were ground into a fine powder by using a pestle and a mortar, and total RNA was extracted using an SV Total RNA Isolation System (Promega) according to the manufacturer's instructions. Contaminating chromosomal DNA in the RNA samples was eliminated by treating with DNase I (Promega). The quantity and quality of RNA samples were assessed by measuring the A_{260} and A_{280} of the samples using Nanodrop (Thermo scientific), and the integrity of the purified RNA samples was determined by denaturing agarose gel electrophoresis.

The purified RNA (2 μg) was used as template to synthesize the first strand cDNA using a SuperScript III First-strand Synthesis System (Invitrogen) with random primers by following the manufacturer's instructions. The resulting cDNA was used as template in a PCR with primers specific for the interested genes and designed to amplify fragments of 100–300 bp (Table S3), and the amplification conditions were as follows: 94 °C for 5 min, and then 30 cycles of 94 °C for 30 s, 58 °C for 30 s, and 72 °C for 30 s, with a final extension at 72 °C for 10 min. To confirm that PCR products were not derived from genomic DNA contaminating the RNA preparations, negative controls were also performed using the sample (lacking reverse transcriptase) as template along with each set of primers.

The quantitative RT-PCR was performed using MaximaTM SYBR Green qPCR Mix (MBI) and an Applied Biosystems 7500 Fast Real-time PCR system. 16S rDNA was used as the internal control. All primers employed are shown in Table S3 of Supporting Information.

3. Results

3.1. Bioinformatic analysis of HmtA, HmtB and HmtD

The genes *hmtA* and *hmtD* are located upstream in the himastatin BGC (Fig. 2). The *hmtA* gene codes for a 247 aa regulator annotated as a MerR family transcriptional regulator on the basis of homologous comparisons (Ma et al., 2011). MerR regulators serve as metal-sensing activators inducing gene expression for elements involved in metal ion homeostasis and efflux in bacteria. These processes enable the cell to differentiate between toxic and essential metals and their elements play a role in eliminating the former and acquiring the latter (Hobman, 2007; Locatelli et al., 2016). However, HmtA shows very low homology with other well-characterized MerR type regulators involved in metal responses for Gram-positive or Gram-negative bacteria, such as: KasV from *S. microaureus* (identity 6%; similarity 10%) (Zhu et al., 2016), SrnR from *S. griseus* (identity 8%; similarity 11%) (Kim et al., 2003), TipAL from *Rhodococcus opacus* (identity 8%; similarity 11%) (Dong et al., 2004) and CueR from *E. coli* (identity 7%; similarity 11%) (Changela et al., 2003). Furthermore, conserved domain analysis of HmtA shows that it contains only a small 62 aa fragmented methylation domain devoid of the usual S-adenosylmethionine (SAM) binding site. HmtA also does not possess the typical metal-binding domain or even the critical DNA binding domain (Changela et al., 2003; Hobman, 2007) characteristic of other MerR family members (Fig. S1).

The *hmtB* gene locates between *hmtA and htmD* and encodes a kinase annotated as acetylglutamate kinase (NAGK) (Ma et al., 2011). Acetylglutamate kinase is the second enzyme in the biosynthetic pathway to L-Arginine. NAGK catalyzes the controlling step of *N*-acetyl glutamate phosphorylation and is feedback inhibited by the final product L-Arginine. NAGK thereby serves in large part to regulate the needs of aa biosynthesis against those of aa utilization (Llacer et al., 2007; Yang, 2017). Conserved domain analyses reveal that HmtB contains the conserved acetylglutamate kinase and amino acid kinase family sequence and structure, showing homology with the structure well-identified NAGKs (Fig. S2), such as: EcNAGK from *E. coli* (identity 27%; similarity 43%) (Ramon-Maiques et al., 2002), ThNAGK from *Thermus thermophilus* (identity 30%; similarity 46%) (Sundaresan et al., 2012), CgNAGK from *Corynebacterium glutamicum* (identity 48%; similarity 60%) (Huang et al., 2016), TmNAGK from *Thermotoga maritima* (identity 32%; similarity 52%) and PaNAGK from *Pseudomonas aeruginosa* (identity 37%; similarity 53%) (Ramon-Maiques et al., 2006). On the strength of these homologies, HmtB appears to be an indirect regulator of aa utilization for himastatin biosynthesis.

Blast analysis results showed that HmtD is a putative regulator or antibiotic biosynthesis protein. In order to further analyze the function of HmtD, another bioinformatic online software ESPript 3.0 was used and the analysis results indicated that HmtD showed high homologue with ParB-a probable chromosome partitioning protein. The HTH motif was resided almost in the middle of HmtD (71–160aa), which was the critical domain for a regulator (Fig. S3). We proposed that HmtD might act as a regulator in the biosynthesis of himastatin based on the above analysis results.

3.2. Identification of HmtD as an activator in himastatin biosynthesis

We applied established λ-RED mediated PCR-targeting mutagenesis to construct three gene insertion mutants: Δ*hmtA*, Δ*hmtB* and Δ*hmtD* for subsequent reverse transcription PCR (RT-PCR) analyses to compare gene expression efficiencies in wild-type (WT) and mutant strains. Following validation of each intended mutation strain

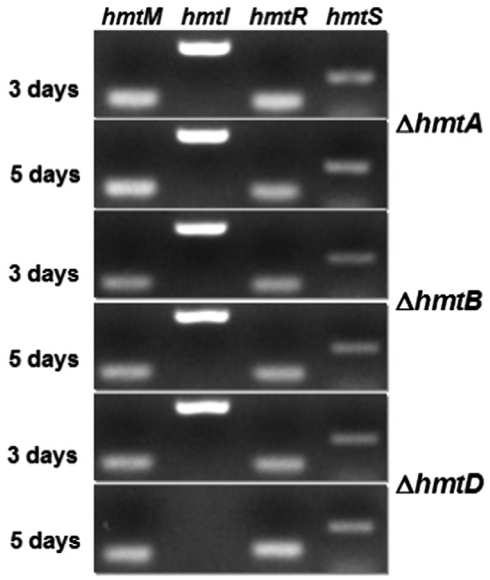

Fig. 3. RT-PCR analysis of Δ*hmtA*, Δ*hmtB* and Δ*hmtD* mutants.

(Figs. S3–5), all mutant strains were cultured in liquid fermentation medium and sampled twice (himastatin biosynthesis initial stage at 3 d and stable stage at 5 d) for mRNA extraction. Differences in specific himastatin biosynthetic gene expression levels, including *hmtI* (himastatin biosynthetic NRPS gene), *hmtM* (precursor biosynthetic gene), *hmtQ* (transporter gene), *hmtS* (P450 like enzyme tailoring gene), were evaluated. Inactivations of *hmtA* and *hmtB* were found to have no direct impact upon the noted *hmt* gene expression efficiencies. There also was no obvious difference in *hmtMQS* expression levels found when evaluating fermentations of the Δ*hmtD* mutant (Fig. 3). Notably, an exception to this was noted with *hmtI*. Inactivation of *hmtD* failed to impact *hmtI* (NRPS) expression at day 3 but induced complete loss of *hmtI* expression by day 5. This dramatic change in putative NRPS machinery indicates that *hmtD* ablation likely rearranges the normal sequence of *hmt* NRPS gene expression events and highlights HmtD as an essential activator involved in timing the himastatin NRPS machinery for efficient hexapeptide monomer assembly.

3.3. Identification of HmtA and HmtB as two repressors involved in regulating himastatin biosynthetic gene expression

Inactivations of *hmtA* and *hmtB* both failed to impact expression efficiencies of required himastatin biosynthetic genes. For subsequent precise analysis of related gene expression level changes during himastatin biosynthesis we employed quantitative RT-PCR to monitor the previously selected genes *hmtIMQS* during day 4 of himastatin biosynthesis. Notably, all four selected expression levels increased significantly by ≈ 9.1-fold, 7.2-fold, 4.6-fold and 4.7-fold, respectively in the Δ*hmtA* mutant strain (Fig. 4). These dramatic changes confirmed that HmtA serves as a negative regulator (repressor) of himastatin biosynthesis. Similarly, inactivation of *hmtB* led to dramatically improved expression of *hmtIQS* as reflected by increases of ≈ 6.2-fold, 9.3-fold and 5.2-fold, respectively, relative to the WT strain (Fig. 4). These findings make clear that HmtB joins HmtA as a vital and powerful repressor in himastatin biosynthesis.

3.4. Enhancement of himastatin bioproduction by inactivating the two atypical repressor ecoding genes: hmtA and hmt B

Given the potential utility of HmtA and HmtB, we sought to generate a high yielding himastatin bioproducing strain via regulatory networks engineering. We fermented the Δ*hmtA* and Δ*hmtB* mutant strains alongside the WT strain (as a control) in 250 mL flasks filled

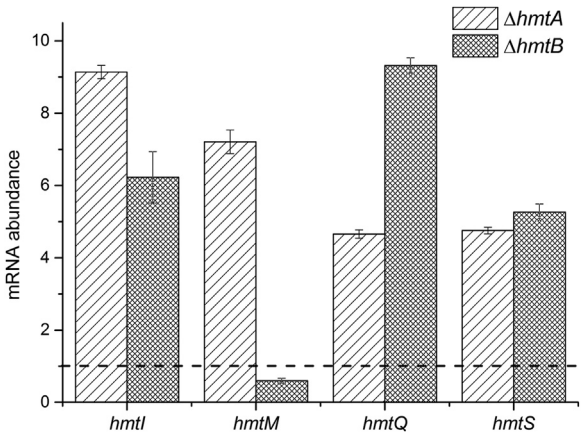

Fig. 4. The qPCR analysis of himastatin biosynthesis-related genes : *hmtIMQS* expression during fermentation of Δ*hmtA* and Δ*hmtB* mutants at day 4. The dashed horizontal line indicates mRNA abundance levels for the WT strain under the same conditions.

with 50 mL hmt medium at 30 °C on a rotary shaker at 200 rpm. After 7 d of shaking cultivation, the medium was harvested and extracted with 100 mL ethyl acetate and the organic solvent then removed under reduced pressure. The remaining extract was then re-dissolved in 1 mL methanol and subjected to HPLC analyses to determine the himastatin titer (Fig. S7). From HPLC analyses it was determined that the engineered strains, Δ*hmtA* and Δ*hmtB*, afforded 9.9-folds and 15.8-folds more himastatin than did the WT "control" strain (Fig. 5). The titers of the himastatin bioproduction in Δ*hmtA* and Δ*hmtB* are 19.02 ± 1.2 μg/mL and 30.40 ± 0.83 μg/mL respectively, compared to those of 1.92 ± 0.09 μg/mL in the wild type (Fig. 6). On the basis of these data it became clear that HmtA and HmtB serve as inhibitors of himastatin biosynthesis; their ablation represents a clearly effective means of generating high yielding himastatin producing strains able to play a central role in advancing preclinical studies of this anti-microbial and anti-tumor natural product.

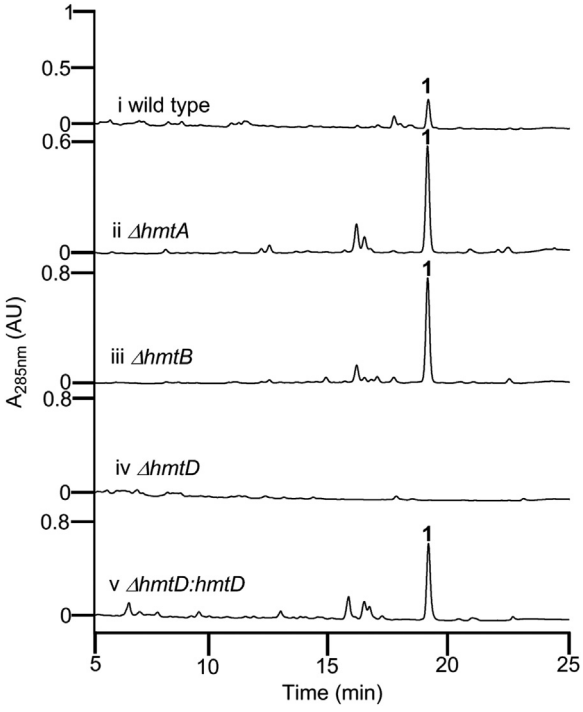

Fig. 5. HPLC analyses of fermentation broths (each individual trial shown). (i), wild type *S. hygroscopicus* ATCC 53653; (ii), Δ*hmtA* mutant (diluted 10 fold); (iii), Δ*hmtB* mutant (diluted 10 fold); (iv), Δ*hmtD* mutant; (v), Δ*hmtD*::*hmtD*, the complementation mutant of Δ*hmtD*, **1**: himastatin.

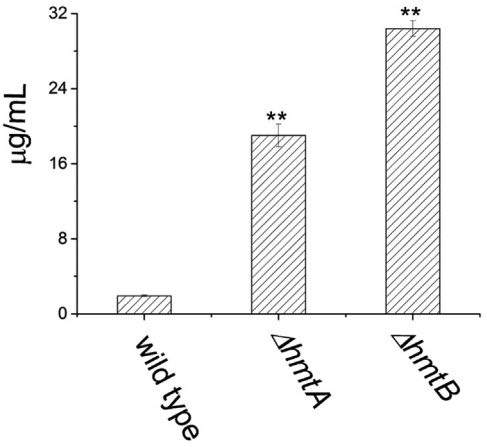

Fig. 6. The titers of himastatin in *S. hygroscopicus* ATCC53653 (wild type), Δ*hmtA* and Δ*hmtB* mutants, respectively ($p < 0.05$*, $p < 0.01$**).

4. Discussion

Streptomyces continue to be a promising resource for mining novel and functional secondary metabolites. Recent progress in genome sequencing has provided new insights into the structural diversity and uniqueness inherent to BGC encoded natural products. Advances in genomic analysis enabled us to identify three regulatory genes: *hmtA*, *hmtB* and *hmtD* distributed within the upstream region of the himastatin BGC. These genes encode three atypical regulators HmtABD lacking the usual DNA binding functions or clearly defined regulatory mechanisms inherent to established homologs; this deviation from precedence has dramatically expanded our insights to secondary metabolism regulation.

As the first regulator identified in the *hmt* cluster bioinformatics revealed HmtD to be a distinct protein lacking any readily identifiable conserved domain. Its identification via qPCR assays and subsequent analyses revealed HmtD to be most intimately associated with construction of the himastatin peptide backbone. Gene inactivation experiments revealed a clear and very strong time-dependent correlation HmtD to *hmtI* expression. This correlation strongly supports the notion that HmtD serves as an activator of himastatin biosynthesis via regulation of *hmtI* (NRPS) expression (Fig. 3).

Despite the absence of any of the usually observed conserved aa sequences or domains expected of MerR family transcriptional regulators, HmtA was annotated as a putative member of this family. While the gene expression confirmed its unforeseen repressed regulation role. Inactivation of *hmtA* revealed its clear albeit unforeseen, role as a regulatory suppressor gene. Indeed, the aforementioned insufficient regulators, without full functional domains, indicated that regulation of the himastatin biosynthetic pathway may not involve an isolated regulatory pathway. We posited that both of these unusual regulators might cooperate with other functional chaperones to maintain stable himastatin bioproduction.

HmtB was found to have relatively high homology to typical bacterial NAGKs and was thus annotated as an NAGK. As the conserved arginine biosynthetic enzyme, NAGKs are subject to feedback inhibition by arginine in many bacteria; this is central to ensuring cellular homeostasis and sustainable processes related to nutrition (Huang et al., 2016; Ramon-Maiques et al., 2006). NAGKs have not, until now, been noted as regulators of secondary metabolism. Our efforts here clearly implicate HmtB, a clearly conserved NAGK, as a repressor of himastatin biosynthesis in *Streptomyces hygroscopicus* ATCC 53653. Our efforts related to HmtB also indicate that steps in himastatin bioproduction may overlap with primary metabolism in the himastatin producer to maintain the utilization of nutrient and amino acid precursor.

The cyclopeptide nature of himastatin suggests that its biosynthesis is nutritionally very costly, placing a high demand especially upon amino acid pools. Accordingly, one means by which HmtA and HmtB may express regulatory influence is to restrict the availability of nutrients for himastatin construction so as to avoid placing an undue burden upon essential primary metabolic pathways. This logic assigns HmtA and HmtB himastatin biosynthetic repressor roles; inactivation of one or both species would remove one or more bottlenecks enabling enhanced himastatin production. Predicated on this idea, we constructed Δ*hmtA* and Δ*hmtB* mutants of *S. hygroscopicus* ATCC 53653; dramatically improved titers of himastatin were noted for both mutant strains validating hypotheses about the repressor roles of HmtA and HmtB while at the same time laying the foundation for more aggressive preclinical studies and industrial production motifs for this interesting therapeutic candidate.

5. Conclusion

In this study we have identified the roles of HmtABD in himastatin biosynthetic pathway. HmtA and HmtD, without any structurally distinct features, were shown to play important repressive and stimulatory roles in himastatin biosynthesis, respectively. And HmtB encodes a new conserved acetylglutamate kinase type repressor in himastatin biosynthesis. Base on repressive networks engineering, the limiting functions of HmtA and HmtB along with the activating functions of HmtD have been identified by gene activation, qPCR, RT-PCR and HPLC studies of gene inactivated mutant strains. Enabled by the discovery and application of two critical repressors HmtA and HmtB, we constructed two new himastatin high-producing mutant strains (Δ*hmtA* and Δ*hmtB*) produced himastatin in titers (19.02 ± 1.2 μg/mL, 9.9 folds and 30.40 ± 0.83 μg/mL, 15.8-folds) much greater than the wild type (WT) producer. Consequently, our effort highlighted not only a new insight into secondary metabolic regulatory mechanisms, but also an approach to safely and efficiently improving metabolite production processes in *Streptomyces*.

Funding

This work was supported in part by a joint fund of National Natural Science Foundation of China and Natural Science Foundation of Guangdong Province (U1501223), the National Natural Science Funds for Distinguished Young Scholar (81425022), the Chinese Academy of Sciences Foundation (XDA11030403), the team project of Guangdong Natural Science Foundation (2016A030312014) and the Special Support Program for Training High-Level Talents in Guangdong (201528018).

Appendix A. Supporting information

Supplementary data associated with this article can be found in the online version at doi:10.1016/j.mec.2018.e00084.

References

Baltz, R.H., 2016. Genetic manipulation of secondary metabolite biosynthesis for improved production in *Streptomyces* and other actinomycetes. J. Ind. Microbiol. Biotechnol. 43, 343–370.

Bibb, M.J., 2005. Regulation of secondary metabolism in streptomycetes. Curr. Opin. Microbiol. 8, 208–215.

Changela, A., Chen, K., Xue, Y., Holschen, J., Outten, C.E., O'Halloran, T.V., Mondragon, A., 2003. Molecular basis of metal-ion selectivity and zeptomolar sensitivity by CueR. Science 301, 1383–1387.

Dong, L., Nakashima, N., Tamura, N., Tamura, T., 2004. Isolation and characterization of the Rhodococcus opacus thiostrepton-inducible genes tipAL and tipAS: application for recombinant protein expression in *Rhodococcus*. FEMS Microbiol. Lett. 237, 35–40.

Du, Y.-L., He, H.-Y., Higgins, M., Ryan, K., 2017. A heme-dependent enzyme forms the nitrogen-nitrogen bond in piperazate. Nat. Chem. Biol., 2411. http://dx.doi.org/10.1038/NCHEMBIO.

Hobman, J.L., 2007. MerR family transcription activators: similar designs, different specificities. Mol. Microbiol. 63, 1275–1278.

Huang, Y.-Y., Li, C., Zhang, H., Liang, S.L., Han, S.Y., Lin, Y., Yang, X.-R., Zheng, S.-P., 2016. Monomeric *Corynebacterium glutamicum* N-acetyl glutamate kinase maintains sensitivity to L-arginine but has a lower intrinsic catalytic activity. Appl. Microbiol. Biotechnol. 100, 1789–1798.

Kamenecka, T.M., Danishefsky, S.J., 1998a. Studies in the total synthesis of himastatin: a revision of the stereochemical assignment. Angew. Chem. Int. Ed. 37, 2993–2995.

Kamenecka, T.M., Danishefsky, S.J., 1998b. Total synthesis of himastatin: confirmation of the revised stereostructure. Angew. Chem. Int. Ed. 37, 2995–2998.

Kamenecka, T.M., Danishefsky, S.J., 2001. Discovery through total synthesis: a retrospective on the himastatin problem. Chemistry 7, 41–63.

Kim, J.-S., Kang, S.-O., Lee, J.-K., 2003. The protein complex composed of nickel-binding SrnQ and DNA binding motif-bearing SrnR of *Streptomyces griseus* represses sodF transcription in the presence of nickel. J. Biol. Chem. 278, 18455–18463.

Kumar, Y., Goodfellow, M., 2008. Five new members of the *Streptomyces violaceusniger* 16S rRNA gene clade: *Streptomyces castelarensis* sp. nov., comb. nov., *Streptomyces himastatinicus* sp. nov., *Streptomyces mordarskii* sp. nov., *Streptomyces rapamycinicus* sp. nov. and *Streptomyces ruanii* sp. nov. Int. J. Syst. Evol. Microbiol. 58, 1369–1378.

Lam, K.S., Hesler, G.A., Mattei, J.M., Mamber, S.W., Forenza, S., Tomita, K., 1990. Himastatin, a new antitumor antibiotic from *Streptomyces hygroscopicus*. I. Taxonomy of producing organism, fermentation and biological activity. J. Antibiot. 43, 956–960.

Leet, J.E., Schroeder, D.R., Krishnan, B.S., Matson, J.A., 1990. Himastatin, a new antitumor antibiotic from *Streptomyces hygroscopicus*. II. Isolation and characterization. J. Antibiot. 43, 961–966.

Leet, J.E., Schroeder, D.R., Golik, J., Matson, J.A., Doyle, T.W., Lam, K.S., Hill, S.E., Lee, M.S., Whitney, J.L., Krishnan, B.S., 1996. Himastatin, a new antitumor antibiotic from *Streptomyces hygroscopicus*. III. Structural elucidation. J. Antibiot. 49, 299–311.

Li, L., Zheng, G.-S., Chen, J., Ge, M., Jiang, W.-H., Lu, Y.-H., 2017. Multiplexed site-specific genome engineering for overproducing bioactive secondary metabolites in actinomycetes. Metab. Eng. 40, 80–92.

Llacer, J.L., Contreras, A., Forchhammer, K., Marco-Marin, C., Gil-Ortiz, F., Maldonado, R., Fita, I., Rubio, V., 2007. The crystal structure of the complex of P-II and acetylglutamate kinase reveals how P-II controls the storage of nitrogen as arginine. Proc. Natl. Acad. Sci. USA 104, 17644–17649.

Locatelli, F.M., Goo, K.S., Ulanova, D., 2016. Effects of trace metal ions on secondary metabolism and the morphological development of streptomycetes. Metallomics 8, 469–480.

Ma, J.-Y., Wang, Z.-W., Huang, H.-B., Luo, M.-H., Zuo, D.-G., Wang, B., Sun, A.-J., Cheng, Y.-Q., Zhang, C.-S., Ju, J.-H., 2011. Biosynthesis of himastatin: assembly line and characterization of three cytochrome P450 enzymes involved in the post-tailoring oxidative steps. Angew. Chem. Int. Ed. 50, 7797–7802.

Martin, J.F., Liras, P., 2010. Engineering of regulatory cascades and networks controlling antibiotic biosynthesis in *Streptomyces*. Curr. Opin. Microbiol. 13, 263–273.

Mendes, M.V., Tunca, S., Anton, N., Recio, E., Sola-Landa, A., Aparicio, J.F., Martin, J.F., 2007. The two-component phoR-phoP system of *Streptomyces natalensis*: inactivation or deletion of phoP reduces the negative phosphate regulation of pimaricin biosynthesis. Metab. Eng. 9, 217–227.

Olano, C., Lombo, F., Mendez, C., Salas, J.A., 2008. Improving production of bioactive secondary metabolites in actinomycetes by metabolic engineering. Metab. Eng. 10, 281–292.

Ramon-Maiques, S., Marina, A., Gil-Ortiz, F., Fita, I., Rubio, V., 2002. Structure of acetylglutamate kinase, a key enzyme for arginine biosynthesis and a prototype for the amino acid kinase enzyme family, during catalysis. Structure 10, 329–342.

Ramon-Maiques, S., Fernandez-Murga, M.L., Gil-Ortiz, F., Vagin, A., Fita, I., Rubio, V., 2006. Structural bases of feed-back control of arginine biosynthesis, revealed by the structures of two hexameric N-acetylglutamate kinases, from *Thermotoga maritima* and *Pseudomonas aeruginosa*. J. Mol. Biol. 356, 695–713.

Sola-Landa, A., Moura, R.S., Martin, J.F., 2003. The two-component PhoR-PhoP system controls both primary metabolism and secondary metabolite biosynthesis in *Streptomyces lividans*. Proc. Natl. Acad. Sci. USA 100, 6133–6138.

Stratigopoulos, G., Cundliffe, E., 2002. Expression analysis of the tylosin-biosynthetic gene cluster: pivotal regulatory role of the tylQ product. Chem. Biol. 9, 71–78.

Stratigopoulos, G., Gandecha, A.R., Cundliffe, E., 2002. Regulation of tylosin production and morphological differentiation in *Streptomyces fradiae* by TylP, a deduced gamma-butyrolactone receptor. Mol. Microbiol. 45, 735–744.

Sundaresan, R., Ragunathan, P., Kuramitsu, S., Yokoyama, S., Kumarevel, T., Ponnuraj, K., 2012. The structure of putative N-acetyl glutamate kinase from *Thermus thermophilus* reveals an intermediate active site conformation of the enzyme. Biochem. Biophys. Res. Commun. 420, 692–697.

van Wezel, G.P., McDowall, K.J., 2011. The regulation of the secondary metabolism of *Streptomyces*: new links and experimental advances. Nat. Prod. Rep. 28, 1311–1333.

Yang, X.-R., 2017. Conformational dynamics play important roles upon the function of N-acetylglutamate kinase. Appl. Microbiol. Biotechnol. 101, 3485–3492.

Zhang, H.-D., Chen, J., Wang, H., Xie, Y.-C., Ju, J.-H., Yan, Y.-J., Zhang, H.-J., 2013. Structural analysis of HmtT and HmtN involved in the tailoring steps of himastatin biosynthesis. FEBS Lett. 587, 1675–1680.

Zhu, C.-C., Kang, Q.-J., Bai, L.-Q., Cheng, L., Deng, Z.-X., 2016. Identification and engineering of regulation-related genes toward improved kasugamycin production. Appl. Microbiol. Biotechnol. 100, 1811–1821.

Zhu, Q.-H., Li, J., Ma, J.-Y., Luo, M.-H., Wang, B., Huang, H.-B., Tian, X.-P., Li, W.-J., Zhang, S., Zhang, C.-S., Ju, J.-H., 2012. Discovery and engineered overproduction of antimicrobial nucleoside antibiotic A201A from the deep-Sea marine actinomycete *Marinactinospora thermotolerans* SCSIO 00652. Antimicrob. Agents Chemother. 56, 110–114.